



Numerical Study of Laminar Natural Convection in an Arch Enclosure Filled with Al₂O₃-Water Based Nanofluid

M. K. Triveni[†], D. Sen and R. Panua

Department of Mechanical Engineering National Institute of Technology, Agartala-799046, India

[†]Corresponding Author Email: triveni_mikky@yahoo.com

(Received March 18, 2015; accepted September 29, 2015)

ABSTRACT

This work numerically investigates the natural convection in an arch enclosure filled with Al₂O₃-water based nanofluid. The left side wall of the enclosure is maintained at a higher temperature than that of right side wall while the remaining walls are kept adiabatic. Two-dimensional steady-state governing equations are solved using the finite volume method (FVM). The present work is conducted to state the effects of pertinent parameters such as nanoparticles volume fraction (ϕ) = 0 to 9%, curvature ratio (CR) = 1 to 1.5 and Rayleigh number (Ra) = 10⁴ to 10⁶ on fluid flow and temperature distribution. The numerical results are presented in the form of streamlines, isotherms, local and average Nusselt number. It is observed from the investigation that the variables are exhibiting a significant impact on the heat transfer. The heat transfer rate is enhanced with the increment in the volume fraction of the nanoparticles up to 5% and after that it is decreased gradually. The heat transfer rate is increased with the increase of curvature ratio and it is significantly higher at CR = 1.5. As per the expectation, the heat transfer is increased along with the increment in Rayleigh number. A good agreement is found between the present work and experimental & numerical results from the literature.

Keywords: Natural convection; Arch enclosure; Nanofluid; Curvature ratio; Nusselt number.

NOMENCLATURE

CR	curvature ratio	<i>Greek symbols</i>	
g	acceleration due to gravity, ms ⁻²	α	thermal diffusivity
H	height of the cavity, m	β	thermal expansion coefficient
Nu _x	Local Nusselt number	θ	dimensionless temperature
Nu	Average Nusselt number	k	thermal conductivity
P	dimensionless pressure	ρ	density
p	pressure, KPa	μ	dynamic viscosity
Pr	Prandtl number	ν	kinematic viscosity
Ra	Rayleigh number	ψ	stream function
T	temperature, K	Ψ	dimensionless stream function
u, v	velocity components, ms ⁻¹	ϕ	volume fraction
U, V	dimensionless velocity component	<i>Subscripts</i>	
W	width of the cavity, m	h	hot wall
x, y	co-ordinates	c	cold wall
X, Y	dimensionless co-ordinates	f	base fluid
		nf	Nanofluid

1. INTRODUCTION

The phenomenon of convection plays an imperative role in the nature as well as in engineering fields due to its wide applications in electronic goods, solar energy collectors, industries, etc. In free convection, water and air are mainly used as a

working medium for heat transfer but the performance of these fluids is often limited because of their low thermal conductivity. However, miniaturization of electronics equipment and increasing industrial needs for process intensification, development of high performance heat transfer fluids has become an interest of numerous investigations in the past few decades. In

order to enhance the thermal conductivity of the base fluid, an innovative technique in which nanoparticles are mixed with the base fluid was introduced by Choi (1995). Later on a plenty of works have been conducted by researchers to signify the effect of different types of nanoparticles on heat transfer rate. Mansour *et al.* (2010) performed a simulation work on mixed convection in a square lid-driven cavity filled with water-based nanofluid containing various types of nanoparticles of Cu, Ag, Al₂O₃ and TiO₂. It was observed that the increase in solid volume fraction was the cause of decrease both the activity of the fluid motion and average Nusselt number. Basak and Chamkha (2012) have done a heat line analysis on natural convection in a square cavity filled with nanofluid. The obtained results were elucidated that the heat transfer rate was enhanced for all nanofluids at Ra = 10⁵ but Alumina-water and Copper-water were exhibited larger enhancement compared to other nanofluids. Oztop and Abu-Nada (2008) have done a numerical work in partially heated rectangular cavity filled with nanofluids. It was reported that the mean Nusselt number was increased with the increase in the volume fraction of nanoparticles and height of the heater for the whole range of Rayleigh number. It was also found that the heat transfer enhancement, using nanofluids, was more pronounced at lower aspect ratio than the higher aspect ratio. Chakma and Abu-Nada (2012) investigated the laminar mixed convection of Al₂O₃-water nanofluid filled in square cavity. The enhancement in the heat transfer rate was found for higher volume fraction of nanoparticles. Ali *et al.* (2013) carried out an experimental analysis on natural convection in a vertical circular enclosure filled with Al₂O₃-water nanofluid. It was observed that the heat transfer coefficient was increased with the increase of volume fraction concentration up to a specific value, and then it is decreased, as the concentration was increased compared to the base fluid, water. Mahmoodi and Sebdani (2012) investigated the free convection in a square cavity filled with Cu-water nanofluid and having an adiabatic square body at the center. It was found that the heat transfer rate was decreased when the size of the adiabatic square body was increased at lower Rayleigh number while for the same case it was found to increase for higher value of Rayleigh number. Rahimi *et al.* (2012) studied the natural convection in a rectangular enclosure filled with a mixture of nanoparticles and water numerically. It was explored that the average Nusselt number was increased with the increase in nanoparticle volume fraction. Ho *et al.* (2008) executed a numerical work on laminar natural convection to exhibit the effect of uncertainties in dynamic viscosity and thermal conductivity of alumina-water nanofluid filled in a square enclosure. The investigation reported that the thermal conductivity and dynamic viscosity of the nanofluid were strongly affected the natural convection heat transfer characteristics. Mahmoodi (2011) conducted a simulation work of natural convection in an L-shaped cavity filled with nanofluid. It was noted that the rate of heat transfer was enhanced with the increase of nanoparticle concentration and

decrease with the increase of the aspect ratio of the cavity. Bhattacharya and das (2015) investigated the natural convection in a square cavity. Results reported that the average Nusselt number was increased with the length of the hot wall and with the increase of Rayleigh number. Sheikhzadeh *et al.* (2012) numerically solved the mixed convection heat transfer in a lid-driven enclosure filled with nanofluids using variable thermal conductivity and viscosity. It was concluded that the average Nusselt number was more sensitive to the viscosity and the thermal conductivity models at low Richardson numbers. Abu-Nada *et al.* (2009) have numerically examined the effects of inclination angle of two-dimensional enclosure filled with Cu-nanofluid. It was found that the effect of nanoparticles concentration on Nusselt number was pronounced more at the low volume fraction than that of higher volume fraction. Aminossadati *et al.* (2011) studied natural convection heat transfer in an isosceles triangular enclosure with a heat source located to the bottom wall and filled with an Ethylene Glycol-Copper nanofluid. The results reported that the heat transfer rate was higher according to the modified Maxwell model. Abu-Nada (2008) investigated the heat transfer rate over a backward facing step using nanofluids. It was observed that for outside recirculation zone, heat transfer rate was enhanced with nanoparticles which were having high thermal conductivity, while within the recirculation zone low thermal conductivity nanoparticles enhanced the heat transfer rate. Bose *et al.* (2013) worked on quadrantal cavity attached with a solid adiabatic fin to the hot wall and filled with water. Investigation reported that the heat transfer and fluid flow is controlled by the solid fin. Mahmoudi *et al.* (2010) examined the natural convection numerically in a square cavity filled with Cu-water nanofluid. The average Nusselt number was increased with the increase in volume fraction. However, it was decreased as the length of the heater increases. Kherief *et al.* (2012) investigated the natural convection numerically in a rectangular cavity in presence of magnetic field. It was concluded that the average nusselt number was enhanced for increasing value of Grashof number while decreased in presence of the magnetic field. Mahmoodi (2011) solved a numerical problem in a square cavity which encompassed with a thin heater and filled with nanofluid. It was found that the horizontal positioned heater was having higher Nusselt number compared to the vertical positioned heater at low Rayleigh number. Also, at high Rayleigh number, Ag-Water nanofluid was more effective to enhance the heat transfer rate. Mahmoodi and hashmei (2012) investigated the heat transfer in a C-shaped enclosure numerically. The outcome of the investigation was reported that the mean Nusselt number was increased with the increase of Rayleigh number, volume fraction of Cu-nanoparticles and was decreased with the increase of the aspect ratio of the cavity. Lai and Yang (2011) used lattice Boltzman method for natural convection heat transfer in a square cavity filled with Al₂O₃-water based nanofluid. Results revealed that the average Nusselt number was increased with the increase of Rayleigh number and

particle volume concentration. Khanafer *et al.* (2003) have numerically investigated the heat transfer enhancement in an enclosure utilizing nanofluids for various pertinent parameters. It was found that the suspended nanoparticles substantially increased the heat transfer rate at any given Grashof number. Abu-Nada *et al.* (2010) worked for heat transfer enhancement in a differentially heated enclosure using variable thermal conductivity and variable viscosity of Al₂O₃–water and CuO–water nanofluids. It was observed that the enclosure with high aspect ratio, experienced more deterioration in the average Nusselt number compared to the enclosures with low aspect ratio. Also, the heat transfer rate was decreased as the volume fractions of both the nanoparticles were increased.

The brief literature survey unfolded that the closed enclosures such as square, rectangular, quadrantal and triangular enclosures filled with air and water have been studied extensively to examine the heat transfer rate. So far, very few works have been done in arch cavity. Hence, the aim of this work is to investigate the fluid flow and heat transfer characteristics in an arch cavity. Many researchers, as mentioned in literature survey, used different types of pure metal and metal oxide nanoparticles such as Cu, Ag, Al, Ti, TiO₂, CuO, SiC, Al₂O₃ etc. with water to enhance the heat transfer rate. While for the present problem Al₂O₃-water based nanofluid is chosen as working fluid for heat transportation because of high sustainability of Al₂O₃ nanoparticles in the fluid. The present work may help the researchers and designers to enhance the heat transfer rate from electronic goods and solar collectors.

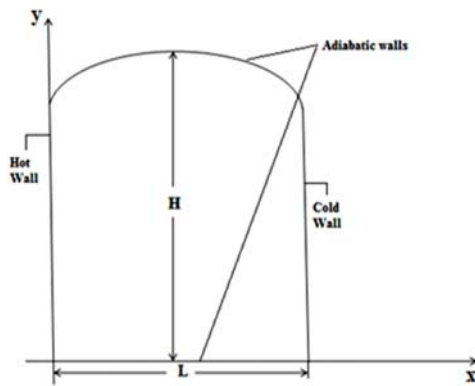


Fig. 1. Schematic diagram of physical domain.

2. DESCRIPTION OF PHYSICAL MODEL AND MATHEMATICAL FORMULATION

Fig. 1 shows the schematic paradigm of an arch cavity along with pertinent boundary conditions. The width of the cavity is considered as L and height H. The curvature ratio (CR = H/L) of the arch cavity is varied from 1 to 1.5. The vertical walls of the cavity are considered as hot and cold walls while bottom and curve walls are considered as adiabatic wall. The cavity is filled with Al₂O₃-

water based nanofluid for heat transport whose physical properties are shown in table 1. Plexiglas is used as an insulating material to prevent the heat leakage from thermally insulated walls.

Table 1 Properties of water and Al₂O₃ nanoparticle at 22°C

Physical Properties	Water	Al ₂ O ₃ nanoparticles
C _p (j/kg k)	4179	765
ρ (kg/m ³)	997.1	3970
k (w/mk)	0.613	25
β × 10 ⁻⁵ (1/k)	21	0.85
d _p (mm)	384	47
μ _f × 10 ⁻³ (Ns/m ²)	0.9576	

Certain assumptions have been made for the present study, which are as follows:

- All walls are impermeable and the effect of radiation is negligible.
- The fluid flow is steady and laminar.
- Gravitational effect is considered in vertical direction.
- All properties of the fluid are constant except density which changes with temperature (as per Boussinesq approximation).

Some important properties of nanofluid such as density, viscosity, thermal conductivity and thermal diffusivity are changed with change in concentration of the volume fractions. All the thermo-physical parameters can be calculated by the formulae presented in table 2.

Table 2 Thermo-physical properties of nanofluid

Density	$\rho_{nf} = (1 - \phi)\rho_f + \phi\rho_{np}$
Heat capacitance	$(\rho C_p)_{nf} = (1 - \phi)(\rho C_p)_f + \phi(\rho C_p)_{np}$
Thermal expansion coefficient	$(\rho\beta)_{nf} = (1 - \phi)(\rho\beta)_f + \phi(\rho\beta)_{np}$
Thermal diffusivity	$\alpha_{nf} = k_{nf}/(\rho C_p)_{nf}$
Thermal conductivity	$\frac{k_{nf}}{k_f} = \frac{k_{np} + (n - 1)k_f - (n - 1)(k_f - k_{np})\phi}{k_{np} + (n - 1)k_f + (k_f - k_{np})\phi}$

Based on assumptions the dimensionless governing equations for natural convection can be written as:

$$\frac{\partial U}{\partial X} + \frac{\partial V}{\partial Y} = 0 \tag{1}$$

$$U \frac{\partial U}{\partial X} + V \frac{\partial U}{\partial Y} = -\frac{\partial P}{\partial X} + Pr \left(\frac{\partial^2 U}{\partial X^2} + \frac{\partial^2 U}{\partial Y^2} \right) \tag{2}$$

$$U \frac{\partial V}{\partial X} + V \frac{\partial V}{\partial Y} = -\frac{\partial P}{\partial Y} + Pr \left(\frac{\partial^2 V}{\partial X^2} + \frac{\partial^2 V}{\partial Y^2} \right) + RaPr\theta \tag{3}$$

$$U \frac{\partial \theta}{\partial X} + V \frac{\partial \theta}{\partial Y} = \left(\frac{\partial^2 \theta}{\partial X^2} + \frac{\partial^2 \theta}{\partial Y^2} \right) \tag{4}$$

Boundary conditions

at the hot wall: $\theta = 1, U = V = 0$ at $X = 0$ and $0 < Y < 1$

at the cold wall: $\theta = 0, U = V = 0$ at $X = 1$ and $0 < Y < 1$ (5)

at the adiabatic walls: $\partial\theta/\partial n = 0, U = V = 0$ at $0 < X < 1$

Using the change of variables

$$X = \frac{x}{H}, Y = \frac{y}{H}, U = \frac{uH}{\alpha_f}, V = \frac{vH}{\alpha_f},$$

$$\theta = \frac{T - T_c}{T_h - T_c}, P = \frac{pH^2}{\rho_{nf}\alpha_f^2}, Pr = \frac{\vartheta_f}{\alpha_f},$$

$$Ra = \frac{g\beta_f(T_h - T_c)H^3}{\alpha_f\vartheta_f} \quad (6)$$

3. NUMERICAL METHODOLOGY

The problem is solved by commercial available software, FLUENT 6.3, which hires finite volume method. The control volume formulations and SIMPLE algorithm coupled with pressure and velocity are used to solve the governing equations (1-4) with the corresponding boundary conditions (5). Momentum and energy equations are discretized by second order upwind technique while the pressure interpolation is done by PRESTO scheme. Solutions are assumed to converge when the following convergence criterion is satisfied at every point in the solution domain:

$$\left| \frac{\theta_{new} - \theta_{old}}{\theta_{new}} \right| \leq 10^{-6} \quad (7)$$

where \square represent primary variables U, V, P, and θ .

The heat transfer coefficient in term of the local Nusselt number is expressed as:

$$Nu_x = \frac{hx}{k} = -\frac{k_{nf}}{k} \frac{\partial\theta}{\partial n} \quad (8)$$

where h is heat transfer coefficient, θ is dimensionless temperature and n denotes normal direction to the plane.

The average Nusselt number along with the hot wall can be written as:

$$Nu = \frac{1}{H} \int_0^H Nu_x dY \quad (9)$$

4. GRID INDEPENDENCY TEST AND VALIDATION

A uniform grid structure in arch cavity is shown in Fig 2. In this study, five different grid sizes (41×41, 51×51, 61×61, 71×71 and 81×81) are adopted to check the independency on mesh. A detailed grid independency test is performed for average Nusselt number at $Ra = 1 \times 10^5$ and $\phi = 0.05$. The table 3 elucidates that the relative errors for the average Nusselt number which is found very less for grid sizes 51×51 and 61×61 compare to others. Since, at high grid size solution may take more time to converge the solution for the same accuracy level. Hence, 51×51 grids adopted for computational time limits.

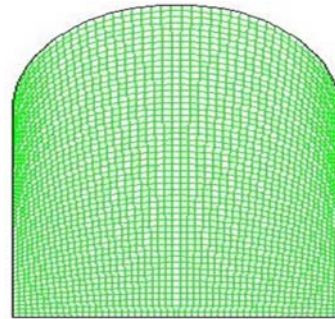


Fig. 2. Recommended uniform Grid structure for arch cavity.

Table 3 Relative error at different grid size

Grid size	Nu	Relative Error
41×41	4.879	
51×51	4.894	0.31%
61×61	4.897	0.061%
71×71	4.881	0.33%
81×81	4.893	0.25%

The present work is validated with the numerical results of Khanafer (2003) and Abu – Nada and experimental results of Krane and Jesse (1983) at $Ra = 10^5$ and $Pr = 0.7$. The presented result shows quite good agreement with the published numerical and experimental results.

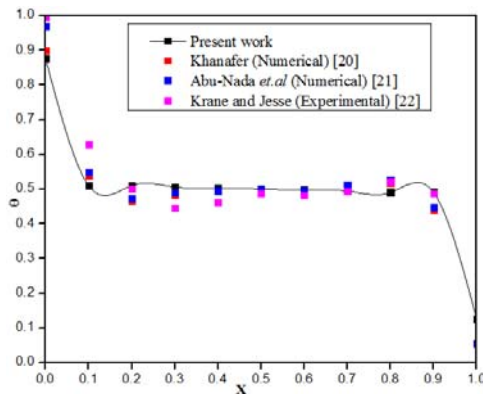


Fig. 3. Comparison between present work and other published data for temperature distribution along the width of the enclosure for nanofluid ($Ra = 1 \times 10^5$ and $Pr = 0.7$).

5. RESULTS AND DISCUSSIONS

The results for free convection in arch enclosure filled with Al_2O_3 -water based nanofluid are drawn for different parameters as Rayleigh number 10^4 to 10^6 , curvature ratio 1 to 1.5 and volume fraction (0 to 9%). The parametric study has been carried out by numerical computation and illustrates it by substantial parameter as streamlines and isotherms.

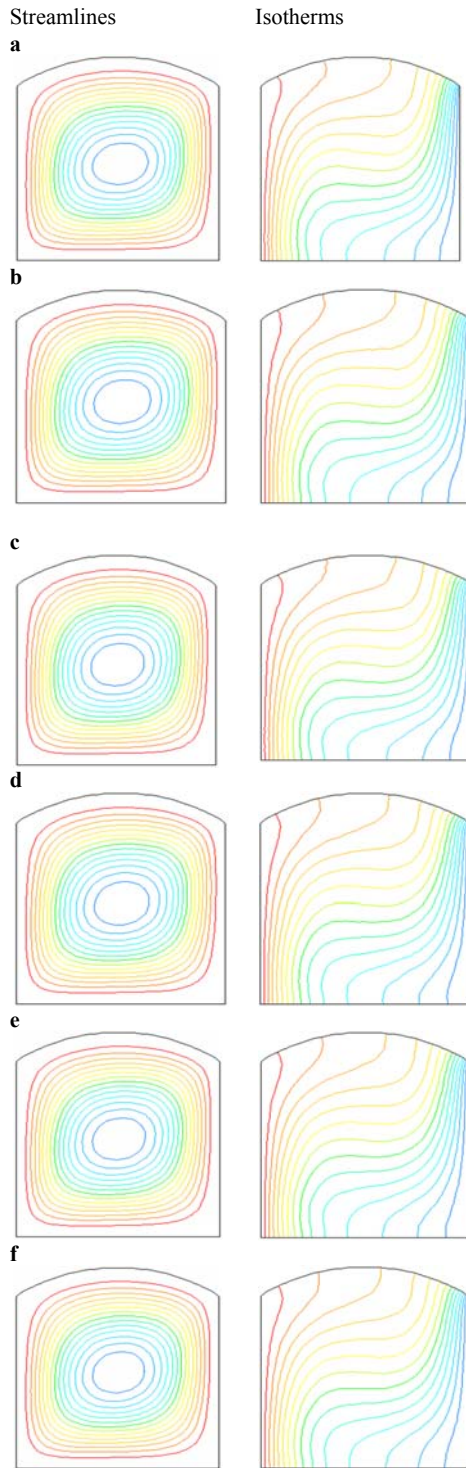


Fig. 4. Streamlines (left) and Isotherms (right) for $Ra = 1 \times 10^4$ and $CR = 1$ at a) $\phi = 0\%$, b) $\phi = 1\%$, c) $\phi = 3\%$, d) $\phi = 5\%$, e) $\phi = 7\%$ and f) $\phi = 9\%$.

5.1 Flow structure and Isotherms

5.1.1 Effect of Volume Fractions

Figs 4 (a) – (f) show the effect of ϕ on the contours of streamlines and isotherms at $Ra = 1 \times 10^4$ and CR

$= 1.17$. It is observed that the fluid moves from the left side of the cavity to right side in a clockwise motion. The streamlines are looked qualitatively quite similar for different volume fractions. But, the intensity of flow is being sluggish as the concentration of nanoparticles is increased. It is happened because the fluid becomes more viscous as the fractions of nanoparticles are increased in the fixed base fluid. As the volume fraction of the nanoparticles is increased the thermal conductivity of the nanofluid is increased. But, the convection coefficient ($hr = h_{nanofluid}/h_{base\ fluid}$) of the nanofluid, shown in Fig. 5, is increased as well. The heat transfer coefficient is highly sensible between 0 to 1% on nanoparticle volume fractions and after that it is increased slowly. This reluctance in the convective heat transfer coefficient indicates that the conduction is dominated over convection heat transfer with the increase of nanoparticles concentration due to which the heat transfer rate is getting reduced. The isotherms contours are distributed throughout the whole cavity and become parallel nearer the thermally active walls. Hardly any changes are observed in the isotherm plots which indicate that the increment in the nanoparticles do not affect the path of heat flow.

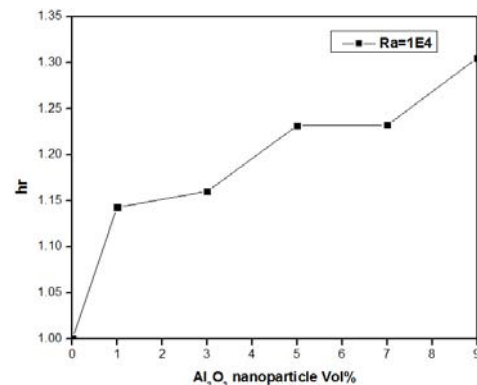


Fig. 5. Effect of Al_2O_3 nanoparticle concentration on convective heat transfer coefficient at $Ra = 10^4$.

5.1.2 Effect of Curvature Ratio

Figs. 6 a-d illustrate the variation in streamlines and thermal plumes at a different curvature ratio for $Ra = 1 \times 10^5$ and $\phi = 3\%$. At $CR = 1$, the streamlines are distributed throughout the cavity and is in an oval shape at the center. The streamlines are parallel to the adiabatic walls. As the curvature ratio is increased the left side diameter of the oval shaped streamline at the center is amplified. It is moved nearer to the bottom adiabatic wall and consequently it is departed from the upper adiabatic wall. This signifies that the increase incurvature ratio affects the flow structure of the fluid and hence the flow is concentrated more between the hot and cold walls. It can be readily perceived from the isotherm lines. The isotherms are dispersed throughout the cavity at lower CR . The thermal boundary lines are shifted from arch adiabatic wall to the upper corner of the cold wall as the curvature

ratio is increased. Hence, it is clear that the convection current and heat transfer rate are mounted with the increase of CR.

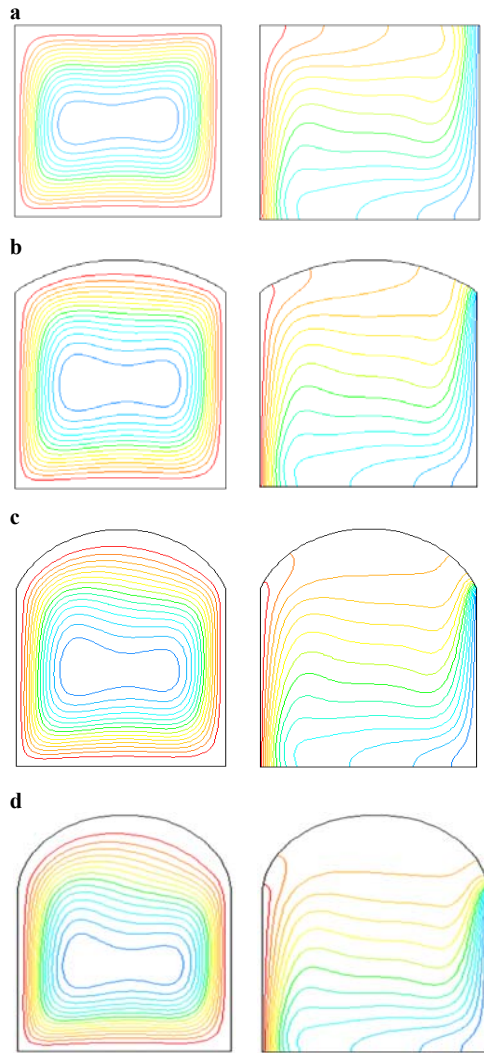


Fig. 6. Streamlines (left) and Isotherms (right) for $Ra = 1 \times 10^5$ and at a) $CR = 1$, b) $CR = 1.17$, c) $CR = 1.33$ and d) $CR = 1.5$.

5.1.3 Effect of Rayleigh Number

Fig. 7 displays the effect of Rayleigh number at curvature ratio 1.5 and $\phi = 5\%$ on streamlines and isotherms. At lower Rayleigh number as shown in Fig. 7a, the streamlines are concentrated away from the active wall and getting circular shaped at the center. As the Rayleigh number is increased to $Ra = 10^5$, the central cell of the streamline get turned into the oval shape and later on it is turned into the irregular shape. However, the streamlines are started circulating closer to the hot and cold walls. Corresponding isotherms contours are dispersed though out the cavity at lower Rayleigh number. But, with the increase of Rayleigh number, these shifted are towards the cold wall and become quite

parallel at the center of the cavity. It indicates that the increment in Rayleigh number intensify the buoyancy force and hence it starts dominate over the viscous effect of the fluid.

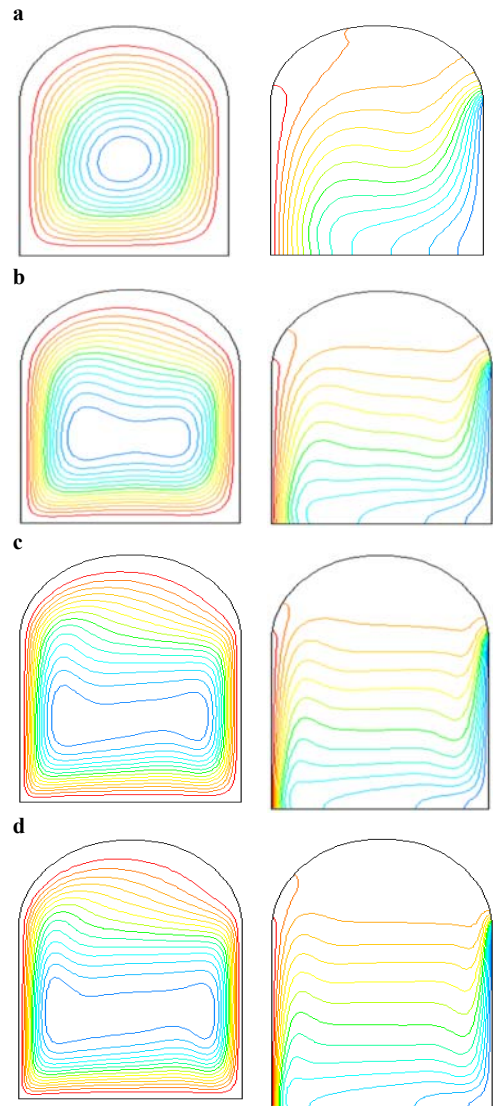


Fig. 7. Streamlines (left) and Isotherms (right) for $CR = 1.5$ and $\phi = 5\%$ at a) $Ra = 1 \times 10^4$, b) $Ra = 1 \times 10^5$, c) $Ra = 5 \times 10^5$ and d) $Ra = 1 \times 10^6$.

5.2 Nusselt Number

5.2.1 Local Nusselt Number (LNN)

Variation of local Nusselt number along with the hot wall is displayed in Fig. 8 a-d for the different curvature ratio at $Ra = 1 \times 10^5$. The graphs are drawn for both pure water and nanofluids with different volume concentrations and compared them with each other. It can be observed from the plots that the local Nusselt number is decreased as the volume concentration of the nanoparticles are increased. The high heat transfer rate is observed between non-dimensional heights 0.1-0.2. Furthermore, the local

Nusselt number decreased with the increase of non-dimensional height of the hot wall. Since, the fluids are getting heated up from the hot wall, is moved up and during the process the fluids are attaining the thermal stability with the height of the hot wall and hence negligible heat transfer is taking place at the top end of the hot wall. The higher peak value of LNN is obtained for water than the nonofluid but the average Nusselt number is found higher for nanofluid than water.

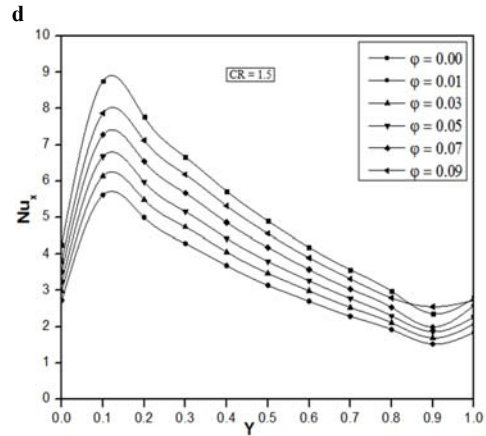
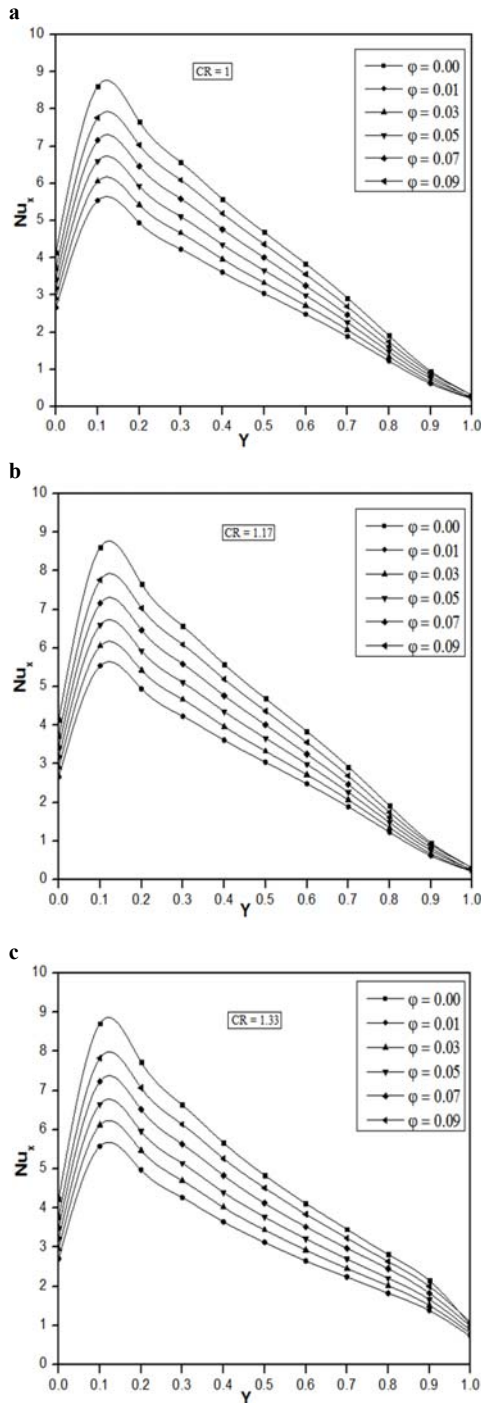


Fig. 8. Variation of local Nusselt number along the hot wall at $Ra = 1 \times 10^5$ for a) CR = 1, b) CR = 1.17, c) CR = 1.33, d) CR = 1.5.

5.2.2 Average Nusselt Number

5.2.2.1 Effect of Volume Fractions

Figs. 9 (a) – (d) demonstrate the effect of solid volume concentration on heat transfer for different size of the enclosure. At $\phi = 1\%$ and $Ra = 10^4$, variation in Nusselt number is observed for CR = 1 to 1.5. From the above observation, it is clear that at low Ra and small volume fraction, the heat transfer rate is increased. Since, higher value of ϕ at low Ra renders the fluid more viscous which reduces the flow velocity. The reduction in velocity tends to reduce the convection current which leads to increase the thickness of the thermal boundary layer. The increment in nanoparticles concentration causes the falling of convective heat transfer which leads to decrease the average Nusselt number. The heat transfer rate is increased with the increase of Ra but decreased with the increase of volume fractions of nanoparticles. Meanwhile, at volume fraction 5% depicts the enhancement in average Nusselt number compare to other volume fractions which are shown in Fig. 9(d). Hence, using of nanoparticles at lower Ra is more beneficial compared to high Ra. Also, water is more suitable at high Rayleigh number.

5.2.2.2 Effect of Curvature Ratio

Fig. 10 portrays the variation in average Nusselt number with the curvature ratio at $\phi = 3\%$ for different Rayleigh number. The enhancement in heat transfer rate is found less for lower curvature ratio. But as the curvature ratio is increased the heat transfer rate is enhanced. Hence, arch cavity with CR= 1.5 is more suitable for application than square and Lower curvature ratio of the cavity.

5.2.2.3 Effect of Rayleigh Number

Fig. 11 depicts the impacts of variation in Rayleigh number on heat transfer rate. The variation in Nu is reported for different curvature ratio of the cavity and for distinct volume fraction. The Rayleigh number is directly related to the temperature gradient. The buoyancy force of the fluid is weak at

lower Rayleigh number because the temperature gradient of the wall is less and hence the energy input to the fluid is low. But as the temperature gradient between the walls is increased the flow rotation of the fluid is also increased and hence a strong buoyancy force is build up inside the cavity which escorts the enhancement of heat transfer rate.

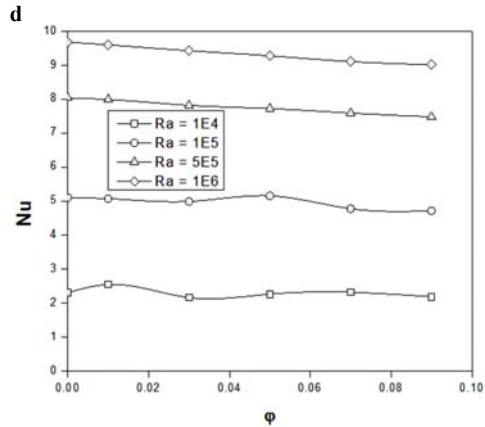
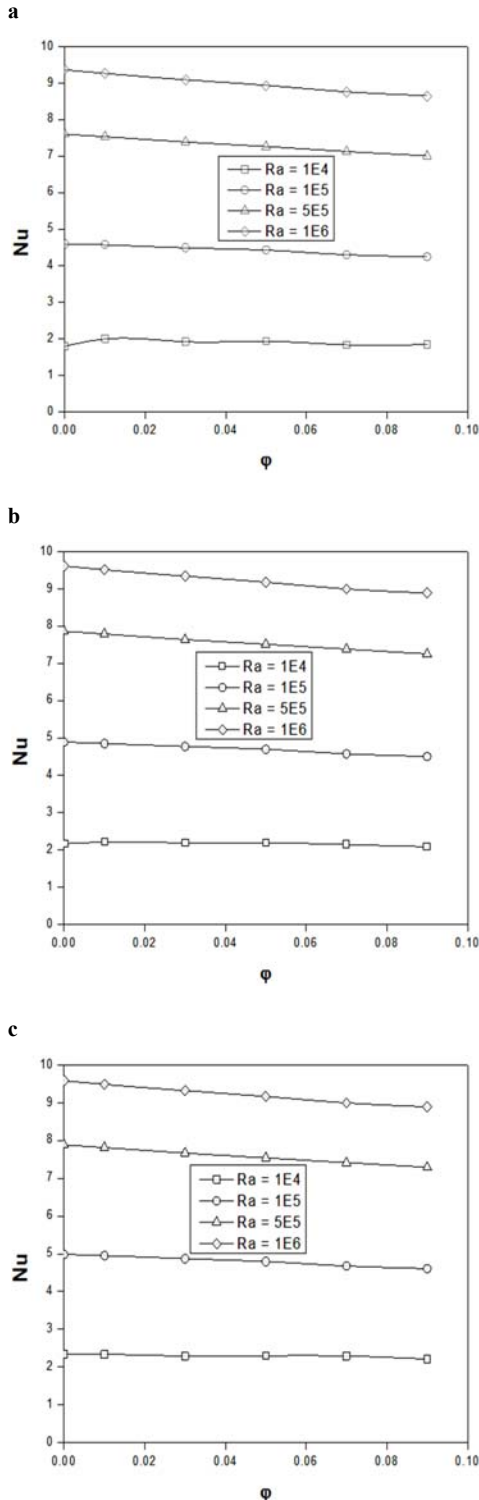


Fig. 9. Average Nusselt number at different volume fractions for a) CR =1, b) CR = 1.16, c) CR = 1.33 and d) CR = 1.5.

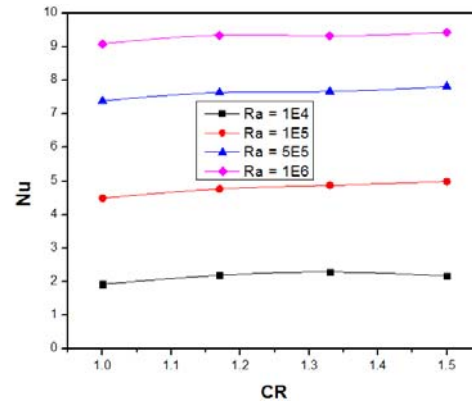


Fig. 10. Variation of average Nusselt number with curvature ratio at fixed $\phi = 3\%$.

6. CONCLUSION

The objective of the current numerical investigation is to study the effect of nanoparticles concentration, curvature ratio and Rayleigh number on the fluid flow and heat transfer characteristic. Finite volume method is used to obtain smooth solutions in terms of streamlines and isotherms for a wide range of Ra and CR. It is observed that the enclosure filled with Al_2O_3 based nanofluid shows a better heat transfer characteristic compared to enclosure filled with pure water. Graphical and tabular results for various parametric conditions are presented and discussed. From this investigation, following conclusions are drawn which are as follows:

1. The enhancement in heat transfer is observed for both water and nanofluid with the increase of CR.
2. The increment in heat transfer rate is observed for the nonparticles concentration up to 5% and after that the average Nusselt number is decreased with the increase of the concentration.

3. The application of Al_2O_3 -water nanofluid is more appealing at lower Rayleigh number rather than the higher. However, the use of water is more beneficial at higher Rayleigh number.
4. The heat transfer rate is increased with the increase in curvature ratio and is found higher at $\text{CR}=1.5$.
5. As per expectation, the average Nusselt number is increased with the increase of Rayleigh number.

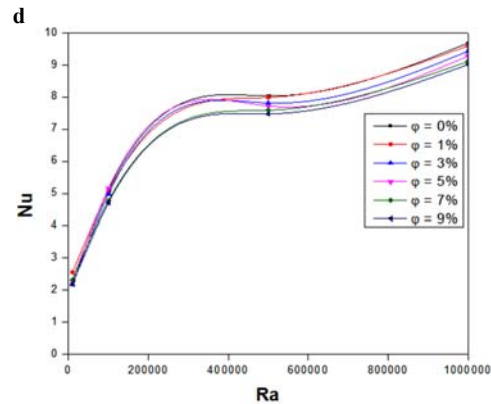
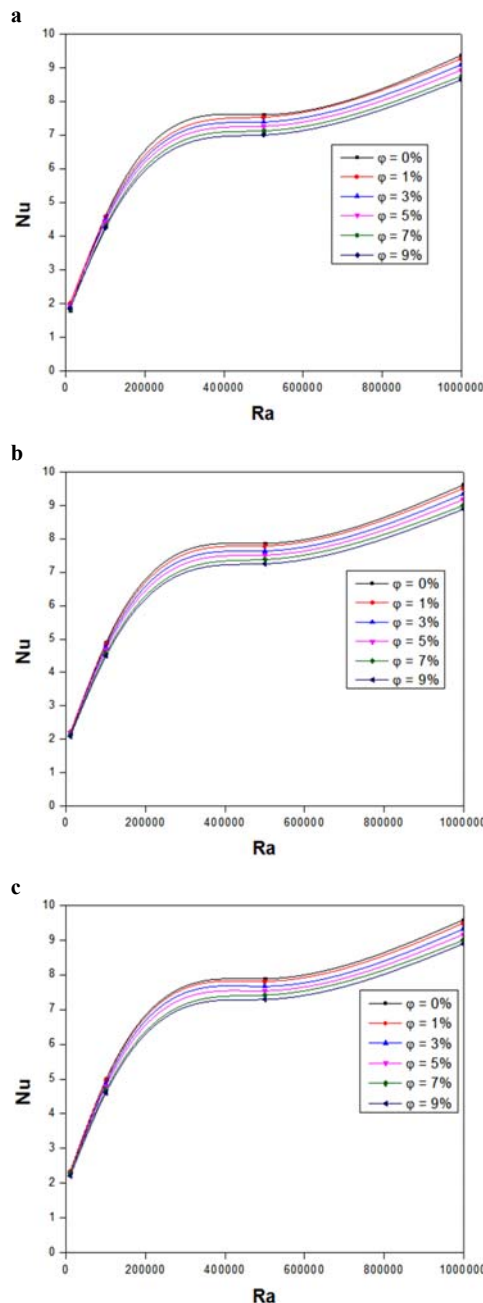


Fig. 11. Variation of average Nusselt number with Rayleigh number for a) $\text{CR}=1$, b) $\text{CR}=1.16$, c) $\text{CR}=1.33$ and d) $\text{CR}=1.5$.

ACKNOWLEDGEMENT

The authors are very grateful to the reviewers for their precious and productive comments.

REFERENCES

- Abu-Nada, E. (2008). Application of nanofluids for heat transfer enhancement of separated flows encountered in a backward facing step. *Int. J. Heat and Fluid Flow* 29, 242-249.
- Abu-Nada, E. and *et al.* (2009). Effects of inclination angle on natural convection in enclosures filled with Cu-water nanofluid. *Int. J. Heat and Fluid Flow* 30, 669-678.
- Abu-Nada, E. and *et al.* (2010). Effect of nanofluid variable properties on natural convection in enclosures. *Int. J. Thermal Science* 49, 479-491.
- Ali, M. and *et al.* (2013). Natural convection heat transfer inside vertical circular enclosure filled with water-based Al_2O_3 nanofluids. *Int. J. Thermal Science* 63, 115-124.
- Aminossadati, S. M. and *et al.* (2011). Enhanced natural convection in an isosceles triangular enclosure filled with a nanofluid. *Computers and Mathematics with Applications* 61, 1739-1753.
- Basak, T. and A. J. Chamka (2012). Heatline analysis on natural convection for nanofluids confined within square cavities with various thermal boundary conditions. *Int. J. Heat and Mass Transfer* 55, 5526-5543.
- Bhattacharya, P. and S. Das (2015). A study on steady natural convection heat transfer inside a square cavity for different values of Rayleigh and nusselt numbers. *Journal of applied Fluid Mechanics* 8(3), 635-640.
- Bose, P. K. and *et al.* (2013). Numerical analysis of laminar natural convection in a quadrantal cavity with a solid adiabatic fin attached to the hot vertical wall. *Journal of Applied Fluid*

- Mechanics* 6(4), 501–510.
- Chakma, A. J. and E. Abu-Nada (2012). Mixed convection flow in single- and double- lid square cavities filled with water-Al₂O₃ nanofluid: effect of viscosity models. *European Journal of Mechanics B/Fluids* 36, 82–96.
- Choi, S. U. S. (1995). Enhancing Thermal Conductivity of Fluids with Nanoparticles. *Development and Applications of Non-Newtonian Flows* 66, 99-105.
- Fluent User's Guide, Release 6.3.26. *Fluent Incorporated* (2005-01-06).
- Ho, C. J. and *et al.* (2008). Numerical simulation of natural convection of nanofluid in a square enclosure: Effects due to uncertainties of viscosity and thermal conductivity. *Int. J. Heat and Mass Transfer* 51, 4506-4516.
- Khanafar, K., K. Vafai and M. Lightstone (2003). Buoyancy-driven heat transfer enhancement in a two-dimensional enclosure utilizing nanofluids. *Int. J. Heat Mass Transfer* 46, 3639–3653.
- Kherief, M. N. and *et al.* (2012). Effects of inclination and magnetic field on natural convection flow induced by a vertical temperature. *Journal of Applied Fluid Mechanics* 5(1), 113–120.
- Krane, R. J. and J. Jessee (1983). Some Detailed Field Measurements for a Natural Convection Flow in a Vertical Square Enclosure. in: *1st ASME-JSME Thermal Engineering Joint Conference* 1, 323–329.
- Lai, F. H. and *et al.* (2011). Lattice Boltzmann simulation of natural convection heat transfer of Al₂O₃/water nanofluids in a square enclosure. *Int. J. Thermal science* 50, 1930-1941.
- Mahmoodi, M. (2011). Numerical simulation of free convection of a nanofluid in L-shaped cavities. *Int. J. of Thermal Sciences* 50, 1731-1740.
- Mahmoodi, M. (2011). Numerical simulation of free convection of a nanofluid in a square cavity with an inside heater. *Int. J. of Thermal Sciences* 50, 2161-2175.
- Mahmoodi, M. (2012). Numerical study of natural convection in C-shaped enclosure. *Int. J. of Thermal Sciences* 50, 76-89.
- Mahmoodi, M. and S. M. Sebdani (2012). Natural convection in a square cavity containing a nanofluid and an adiabatic square block at the center. *Superlattices and Microstructures* 52, 261-275.
- Mahmoudi, A. H., M. Shahi, A. H. Raouf and A. Ghasemian (2010). Numerical study of natural convection cooling of horizontal heat source mounted in a square cavity filled with nanofluid. *Int. Communications in Heat and Mass Transfer* 37, 1135-1141.
- Mansour, M. A. and *et al.* (2010). Numerical simulation of mixed convection flows in a square lid-driven cavity partially heated from below using nanofluid. *Int. Communication in Heat and Mass Transfer* 37, 1504–1512.
- Oztop, H. F. and Abu-Nada, E. (2008). Numerical study of natural convection in partially heated rectangular enclosures filled with nanofluids. *International Journal of Heat and Fluid Flow* 29, 1326–1336.
- Patankar, S. V. (1980). *Numerical Heat Transfer and Fluid Flow*, Taylor & Francis.
- Rahimi, M. and *et al.* (2012). Natural convection of nanoparticle - water mixture near its density inversion in a rectangular enclosure. *Int. Communication in Heat and Mass Transfer* 39, 131-137.
- Sheikhzadeh, G. A. and *et al.* (2012). Numerical study of mixed convection flows in a lid-driven enclosure filled with nanofluid using variable properties. *Results in Physics* 2, 5-13.
- Walid, A. and O. Ahmed (2010). Buoyancy induced heat transfer and fluid flow inside a prismatic cavity. *Journal of Applied Fluid Mechanics* 3(2), 77–86.